Inorg. Chem. **2007**, *46*, 5922–5932

Alkynyl Ruthenium Colorimetric Sensors: Optimizing the Selectivity toward Fluoride Anion

Jean-Luc Fillaut,*,† Julien Andriès,† Johann Perruchon,† Jean-Pierre Desvergne,‡ Loïc Toupet,§ Lotfi Fadel,†,# Bachir Zouchoune,†,# and Jean-Yves Saillard†

UMR 6226 CNRS - Université Rennes 1, "Sciences chimiques de Rennes", Avenue du Général Leclerc, 35042 Rennes, France, UMR 5255 CNRS - Université Bordeaux 1, Institut des Sciences Moléculaires, 351, Cours de la Libération, 33405 Talence, France, UMR 6626 CNRS - Université Rennes 1, Laboratoire de Physique de la Matière Condensée, Université de Rennes 1, 35042 Rennes, France, and Laboratoire de Chimie Moléculaire, du Contrôle de l'Environnement et des Mesures Physico-chimiques, Université Mentouri-Constantine, 25000 Constantine, Algeria

Received December 14, 2006

We report on the synthesis of alkynyl ruthenium colorimetric sensors whose receptors are constituted by thiazolidinedione, rhodanine, or barbituric heads as recognition centers for anions. As modifications in the charge density at these recognition centers affect the whole molecule, through the alkynyl ligand acting as a communicating wire, the effects of hydrogen-bonding interactions with the anions were observed with the naked eye and monitored by UV–vis absorption spectrometry. The selectivity of the sensors was improved through electronic modifications of the alkynyl ruthenium subunit: the higher the electron density at the receptor head, the higher the selectivity is. TD-DFT calculations rationalize the long-range electronic communication as a main characteristic of the alkynyl ruthenium species and as a key to improve the selectivity of alkynyl ruthenium-based sensors toward anions.

Introduction

The design of selective sensors for anions captures intensive interest because of the crucial role played by anions in biological processes, medicine, catalysis, and molecular assembly.[1−4] Among biologically functional anions, fluoride is one of particular importance, owing to its role in dental care and treatment of osteoporosis.[5−7] On the other side, wastewater containing fluoride is released from various industries, such as metal processing, semiconductor, glass, and fine chemicals industries. Finally, fluoride anion is associated with the nerve gas Sarin, which loses a fluoride anion during hydrolysis.[8] As a result, there is a need to develop new selective and sensitive methods for fluoride detection. One of the more attractive approaches in this field is based on colorimetric sensors,[9−12] which generally involve a binding site combined with a chromophore which transduce ion-binding into clearly identified optical signals.

We present herein the design of a new family of colorimetric anion sensors based on alkynyl ruthenium chromophores.[13] These sensors allow a straightforward colorimetric detection of F^- that can discriminate it from, for instance, AcO^-, $H_2PO_4^-$, and HSO_4^- anions. The unique spectral and sensing properties of these ruthenium derivatives were rationalized by TD-DFT calculations.

* To whom correspondence should be addressed. E-mail: jean-luc.fillaut@univ-rennes1.fr.
† Université Rennes 1, "Sciences chimiques de Rennes".
‡ Université Bordeaux 1.
§ Université Rennes 1, Laboratoire de Physique de la Matière Condensée.
# Université Mentouri-Constantine.

(1) Bowman-James, K. *Acc. Chem. Res.* **2005**, *38* (8), 671−678.
(2) Vilar, R. *Angew. Chem., Int. Ed.* **2003**, *42* (13), 1460−1477.
(3) Sambrook, M. R.; Beer, P. D.; Wisner, J. A.; Paul, R. L.; Cowley, A. R. *J. Am. Chem. Soc.* **2004**, *126* (47), 15364−15365.
(4) Seel, C.; de Mendoza, J. *Compr. Supramol. Chem.* **1996**, *2*, 519−552.
(5) Aaseth, J.; Shimshi, M.; Gabrilove, J. L.; Støa Birketvedt, G. *J. Trace Elem. Exp. Med.* **2004**, *17*, 83−92.
(6) Kirk, K. L. *Biochemistry of the Halogens and Inorganic Halides*; Plenum Press: New York, 1991; p 58.
(7) Kleerekoper, M. *End. Metab. Clin. North Am.* **1998**, *27*, 441−452.
(8) Xie, Y.; Popov, B. N. *Anal. Chem.* **2000**, *72*, 2075−2079.
(9) Beer, P. D.; Hayes, E. J. *Coord. Chem. Rev.* **2003**, *240*, 167−189.
(10) Desvergne, J.-P.; Czarnik, A. W. *Chemosensors of Ion and Molecular Recognition*; NATO ASI Series, Kluwer: Dordrecht, The Netherlands, 1997; p 492.
(11) Martinez-Manez, R.; Sancenon, F. *Chem. Rev.* **2003**, *103*, 4419−4476.
(12) Suksai, C.; Tuntulani, T. *Chem. Soc. Rev.* **2003**, *32*, 192−202.
(13) Fillaut, J.-L.; Andriès, J.; Toupet, L.; Desvergne, J.-P. *Chem. Commun.* **2005**, 2924−2926.

10.1021/ic062389i CCC: $37.00
Published on Web 06/29/2007

Scheme 1[a]

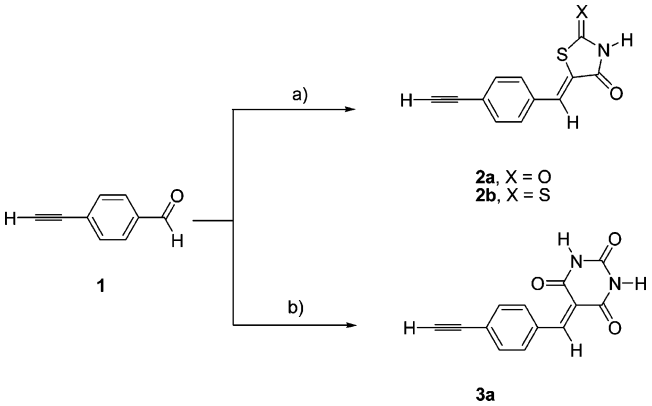

[a] 1 equiv of thiazolidine-2,4-dione (**2a**) or rhodanine (**2b**), acetonitrile, AcOH (ca. 1 equiv), NH_4OAc (0.5 equiv), reflux, 45 min. (b) 1.1 equiv of barbituric acid, EtOH, 65 °C, 20 h.

Alkynyl ruthenium complexes possess an almost linear M−C≡C−R structure and give rise to a long-range electronic coupling between the metal and the remote groups through the π-conjugated pathway. To the best of our knowledge, alkynyl ruthenium complexes have never been considered as sensors for small molecular and ionic species,[14−17] although the incorporation of transition metal subunits has led to the development of several new strategies for molecular recognition.[18,19] Our approach is based on the attachment of hydrogen-bonding recognition sites at the remote end of alkynyl ruthenium derivatives. Modifications in the charge density at these recognition sites affect the whole molecule through the alkynyl ligand acting as a communicating wire. In the present study, rhodanine and barbituric units have been selected as recognition centers; they display one or two NH hydrogen-bond donors surrounded by two neighboring carbonyl groups and thus are new potential candidates for investigating hydrogen-bond formation. We also reveal that the selectivity of these alkynyl ruthenium-based sensors can be improved through electronic modifications of the alkynyl ruthenium moiety.

Results and Discussion

Synthesis. We report on the synthesis of alkynyl ruthenium sensors whose receptors are constituted by thiazolidinedione, rhodanine, or barbituric heads as potential recognition centers. Indeed, we considered two series of compounds: complexes **5** and **6** with a thiazolidinedione or a rhodanine head bear one NH site (Scheme 2); complexes **7**−**10** with a barbituric or thiobarbituric head bear two NH sites per molecule (Schemes 3 and 4). The synthesis of the sensors **5**−**7** and **9a**,**b** was achieved starting from the corresponding alkynes **2** and **3** via a well-established two-step procedure.[20,21] The new acetylenic intermediates required for the syntheses were prepared by a Knoevenagel condensation according to literature procedures (Scheme 1).[22−24] These compounds were characterized by IR, ^1H, ^{13}C and ^{31}P NMR spectroscopy, and mass spectrometry.

The synthetic methodologies employed for the preparation of the ruthenium derivatives have been adapted from previously reported procedures.[21,25] The reaction of acetylenes **2** and **3** and $[Cl(PPh_2CH_2CH_2PPh_2)_2Ru][TfO]$[25,26] in THF at room temperature for 20 h resulted in the formation of vinylidene intermediates. Their complete formation was monitored by ^{31}P NMR spectroscopy. These intermediates were then dissolved in CH_2Cl_2 and filtered to remove the excess of free acetylene before deprotonation with triethylamine (methylene chloride, room temperature, 1 h). The resulting alkynyl compounds were washed with water before being isolated as crystalline powders in ∼65−75% yields.

Similarly, **9a** and **9b** were obtained starting from the thiophene-substituted alkynyl derivatives bearing either a benzylidene barbituric moiety or its dimethylated analogue (Scheme 3).

Using these synthesis methods for **8**, we could not obtain a clean product. Consequently this compound was obtained by a direct Knoevenagel condensation[22] of thiobarbituric acid on *trans*-$(dppe)_2Ru(Cl)(C{\equiv}C{-}C_6H_4{-}CHO)$[15] (dppe = diphenylphosphinoethane) in ethanol at reflux for 1 week (Scheme 2). **8** precipitated during the reaction and can be recovered as a blue powdery solid in 40% yield. **10** was obtained through halide abstraction applied to **7** as a route to cationic nitrile complexes[27,28] (Scheme 4). Indeed, **7** reacted with benzonitrile in the presence of both NH_4PF_6 and NEt_3 in methylene chloride to lead to the rapid formation (less than 1 h at room temperature) of isomerically pure **10.** All the spectroscopic data of compounds **5**−**10** were found to be consistent with their proposed structures. ^{31}P NMR spectra of all complexes contain one singlet resonance, in agreement with the trans geometry at the ruthenium center.

X-ray Structure of 9b. Dark blue crystals of **9b** were obtained upon slow diffusion of a dichloromethane−pentane solution. A plot of the complex molecular structure is shown in Figure 1, and pertinent bond parameters are given in Table 1. The X-ray structure determination of **9b** fully established the nature of this complex. The barbituric fragment is located apart from the envelope of the phosphorus ligands around the metal and is sterically noncrowded. Most bond lengths

(14) Lewis, J. D.; Moore, J. N. *Dalton Trans.* **2004**, 1376−1385.
(15) Siu, P. K. M.; Lai, S. W.; Lu, W.; Zhu, N. Y.; Che, C. M. *Eur. J. Inorg. Chem.* **2003**, 2749−2752.
(16) Yam, V. W. W. *Pure Appl. Chem.* **2001**, *73*, 543−548.
(17) Yang, Q. Z.; Wu, L. Z.; Zhang, H.; Chen, B.; Wu, Z. X.; Zhang, U. P.; Tung, C. H. *Inorg. Chem.* **2004**, *43*, 5195−5197.
(18) Beer, P. D. *Top. Curr. Chem.* **2005**, *255*, 125−162.
(19) Sun, S.-S.; Lees, A. J. *Coord. Chem. Rev.* **2002**, *230*, 171−192.
(20) Touchard, D.; Haquette, P.; Guesmi, S.; LePichon, L.; Daridor, A.; Toupet, L.; Dixneuf, P. H. *Organometallics* **1997**, *16*, 3640−3648.
(21) Touchard, D.; Dixneuf, P. H. *Coord. Chem. Rev.* **1998**, 178−180, 409−429.
(22) Jursic, B. S. *J. Heterocycl. Chem.* **2001**, *38*, 655−657.
(23) Okazaki, M.; Uchino, N.; Ishihara, M.; Fukunaga, H. *Bull. Chem. Soc. Jpn.* **1998**, *71*, 1713−1718.
(24) Tanaka, K.; Chen, X.; Kimura, T.; Yoneda, F. *Chem. Pharm. Bull.* **1988**, *36*, 60−69.
(25) Rigaut, S.; Perruchon, J.; Le Pichon, L.; Touchard, D.; Dixneuf, P. H. *J. Organomet. Chem.* **2003**, *670*, 37−44.
(26) Mantovani, N.; Brugnati, M.; Gonsalvi, L.; Grigiotti, E.; Laschi, F.; Marvelli, L.; Peruzzini, M.; Reginato, G.; Rossi, R.; Zanello, P. *Organometallics* **2005**, *24*, 405−418.
(27) Fillaut, J.-L.; Dua, N. N.; Geneste, F.; Toupet, L.; Sinbandhit, S. *J. Organomet. Chem.* **2006**, *691*, 5622−5630.
(28) Li, Z.; Beatty, A. M.; Fehlner, T. P. *Inorg. Chem.* **2003**, *42*, 5707−5714.

Scheme 2[a]

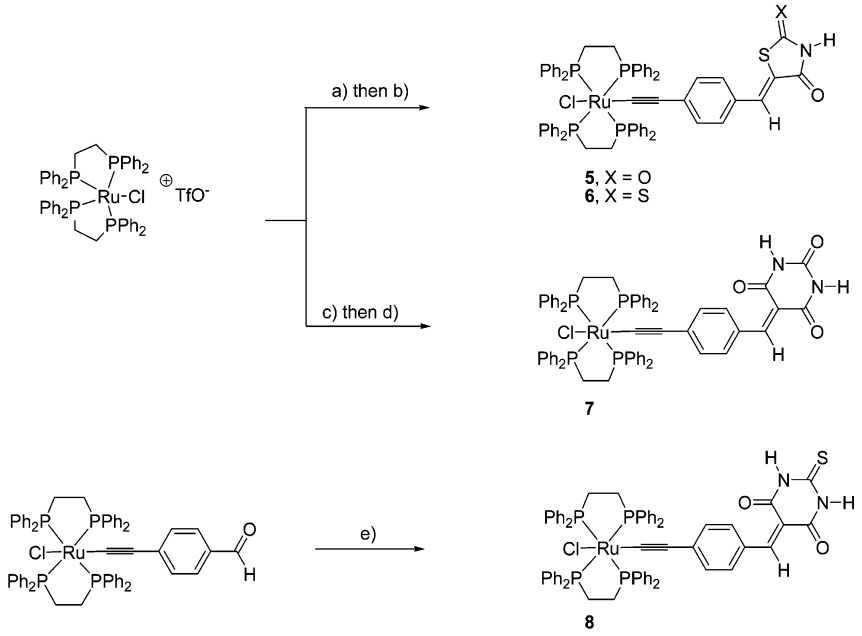

[a] (a) **2a** or **2b** (1.1 equiv), THF−CH_2Cl_2 (5/1, v/v), RT, 20 h. (b) *t*-BuOK (2 equiv), THF, RT, 10 min. (c) **3a** (1.1 equiv), THF, RT, 20 h. (d) NEt_3 (ca. 1.1 equiv), CH_2Cl_2, RT, 1 h. (e) [*trans*-RuCl(dppe)$_2$(C≡C-*p*-C_6H_4−CHO)], thiobarbituric acid (1.5 equiv), THF−EtOH (1/5, v/v), 65 °C, 1 week.

Scheme 3[a]

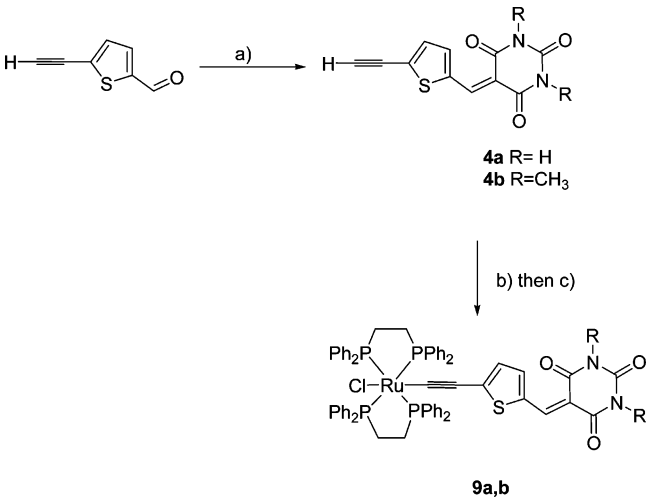

[a] (a) 1 equiv of barbituric acid or dimethylbarbituric acid, EtOH, 65 °C, 20 h. (b) [(dppe)$_2$RuCl]$^+$TfO$^-$, **4a** (1.1 equiv) in THF−CH_2Cl_2 (5/1, v/v) or **4b** (1.1 equiv), in CH_2Cl_2, RT, 20 h. (c) NEt_3 (ca. 1.1 equiv), CH_2Cl_2, RT, 1 h.

and angles about the Cl−Ru−C(1)−C(2)−C(3) units in this structure are standard. For instance, the Cl−Ru (2.5127(6) Å), Ru−C(1) (1.977(2) Å), C(1)−C(2) (1.204(3) Å), and C(2)−C(3) (1.406(3) Å) bond lengths for this complex fall within the range of those previously reported for related octahedral *trans*-bis(bidentate phosphine)ruthenium alkynyl complexes.[29−32] The Ru−C(1) bond length of 1.977(2) Å is short with respect to those typically observed in alkynyl complexes of the same metal entity (1.990−2.078 Å) while the C(1)−C(2) bond of 1.204(3) Å is only slightly longer than a typical C≡C triple bond (average value 1.189 Å). Finally, the C(2)−C(3) distance of 1.406 (3) resembles a single bond between an sp- and an sp^2-hybridized carbon atom.[33] The dihedral angle formed by the planes of the thienyl and barbituric rings is close to coplanarity (10.0° ± 0.1°) (see Table 1), confirming the conjugated pathway from one part of this model to the other. The values (136.1(3)°) for the C−C−C angle at the methine C(7) atom linking these two rings appears at first sight to be wide, but it is consistent with angles previously reported for related organic systems.[34] Actually, the bond angles at C(7) and C(8) indicate that the S−O(3) contact is repulsive and results in a wider C(7)−C(8)−C(11) angle (123.6 (2)°) compared to C(7)−C(8)−C(9) (116.3 (3)°). The 1,3-dimethylpyrimidine-trione ring is nearly planar. Bond lengths and angles in this heterocyclic ring fall within the range of those previously reported for comparable fragments.[34]

Naked Eye Sensing of Anions. The analyte recognition via hydrogen-bonding interactions can be easily followed with the naked eye or by monitoring the changes in the UV−vis absorption spectra of complexes **5**−**10** upon anion addition. Initially, the qualitative estimation of the affinity of the sensors **5**−**9** toward various anions was performed visually (Figure 2). It is noteworthy that, for all these sensors, the observed color changes were fully reversible upon addition of water, which presumably competes with the anions. On the other hand, the color of a methylene chloride

(29) Fillaut, J.-L.; Perruchon, J.; Blanchard, P.; Roncali, J.; Golhen, S.; Allain, M.; Migalsaka-Zalas, A.; Kityk, I. V.; Sahraoui, B. *Organometallics* **2005**, *24*, 687−695.
(30) Hurst, S. K.; Cifuentes, M. P.; Morrall, J. P. L.; Lucas, N. T.; Whittall, I. R.; Humphrey, M. G.; Asselberghs, I.; Persoons, A.; Samoc, M.; Luther-Davies, B.; Willis, A. C. *Organometallics* **2001**, *20*, 4664−4675.
(31) Lebreton, C.; Touchard, D.; Le Pichon, L.; Daridor, A.; Toupet, L.; Dixneuf, P. H. *Inorg. Chim. Acta* **1998**, *272*, 188−196.
(32) Zhu, Y. B.; Millet, D. B.; Wolf, M. O.; Rettig, S. J. *Organometallics* **1999**, *18*, 1930−1938.
(33) Nast, R. *Coord. Chem. Rev.* **1982**, *47*, 89−124.
(34) Rezende, M. C.; Dominguez, M.; Wardell, J. L.; Skakle, J. M. S.; Low, J. N.; Glidewell, C. *Acta. Crystallogr. C* **2005**, *C61*, o306−o311.

Scheme 4[a]

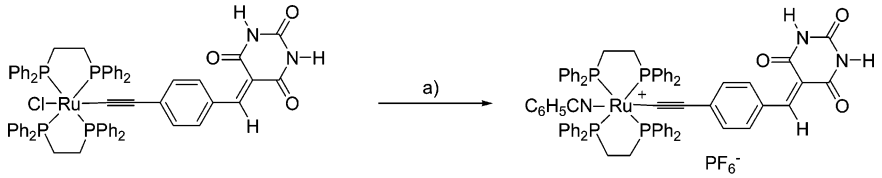

7 **10**

[a] (a) NH_4PF_6 (3.5 equiv), benzonitrile (1.3 equiv), CH_2Cl_2, RT, 20 h.

Table 1. Selected Bond Lengths (Å) and Bond Angles (deg) for **9b**

Bond Lengths [Å]			
Ru(1)−C(1)	1.977(2)	N(1)−C(12)	1.469(4)
Ru(1)−P(2)	2.3791(6)	N(2)−C(10)	1.378(4)
Ru(1)−P(3)	2.3856(6)	N(2)−C(11)	1.403(4)
Ru(1)−P(4)	2.4140(6)	N(2)−C(13)	1.458(4)
Ru(1)−P(1)	2.4270(6)	C(1)−C(2)	1.204(3)
Ru(1)−Cl(1)	2.5127(6)	C(2)−C(3)	1.406(3)
S(1)−C(3)	1.736(3)	C(3)−C(4)	1.386(4)
S(1)−C(6)	1.740(2)	C(4)−C(5)	1.381(4)
O(1)−C(9)	1.218(4)	C(5)−C(6)	1.397(4)
O(2)−C(10)	1.214(4)	C(6)−C(7)	1.411(3)
O(3)−C(11)	1.214(3)	C(7)−C(8)	1.374(4)
N(1)−C(10)	1.374(4)	C(8)−C(11)	1.443(4)
N(1)−C(9)	1.399(4)	C(8)−C(9)	1.471(4)
Angles [deg]			
C(1)−Ru(1)−P(2)	93.43(7)	C(5)−C(4)−C(3)	113.5(2)
C(1)−Ru(1)−P(3)	83.14(6)	C(4)−C(5)−C(6)	114.5(2)
C(1)−Ru(1)−P(4)	85.87(7)	C(5)−C(6)−C(7)	121.2(2)
P(2)−Ru(1)−P(4)	177.38(2)	C(5)−C(6)−S(1)	109.09(18)
C(1)−Ru(1)−P(1)	92.87(6)	C(7)−C(6)−S(1)	129.5(2)
C(1)−Ru(1)−Cl(1)	175.79(6)	C(8)−C(7)−C(6)	136.1(3)
C(3)−S(1)−C(6)	92.63(12)	C(7)−C(8)−C(11)	123.6(2)
C(10)−N(1)−C(9)	124.6(2)	C(7)−C(8)−C(9)	116.3(3)
C(10)−N(1)−C(12)	116.8(3)	C(11)−C(8)−C(9)	120.2(2)
C(9)−N(1)−C(12)	118.5(3)	O(1)−C(9)−N(1)	119.4(3)
C(10)−N(2)−C(11)	124.7(3)	O(1)−C(9)−C(8)	124.4(3)
C(10)−N(2)−C(13)	117.3(3)	N(1)−C(9)−C(8)	116.2(3)
C(11)−N(2)−C(13)	117.9(3)	O(2)−C(10)−N(1)	121.3(3)
C(2)−C(1)−Ru(1)	177.1(2)	O(2)−C(10)−N(2)	121.2(3)
C(1)−C(2)−C(3)	174.0(3)	N(1)−C(10)−N(2)	117.6(3)
C(4)−C(3)−C(2)	129.8(2)	O(3)−C(11)−N(2)	119.0(3)
C(4)−C(3)−S(1)	110.25(19)	O(3)−C(11)−C(8)	124.6(3)
C(2)−C(3)−S(1)	119.9(2)	N(2)−C(11)−C(8)	116.4(2)

solution of the reference compound **9b** was not affected by the addition of anionic species whatever they were, as expected (this compound does not bear NH sites).

Instantaneous color changes were observed upon addition of F^-, AcO^-, or $H_2PO_4^-$ anions to dichloromethane solutions of complexes **5**−**8** and **9a.** Conversely, no detectable color change was observed even upon addition of large excesses of HSO_4^-, Cl^-, Br^-, and NO_3^- to these complexes. A very fast red to yellow anion-induced color change upon addition of few molar equivalents of F^-, AcO^-, or $H_2PO_4^-$ anions was observed for both complexes **5** and **6**. No clear optical distinction between these three anions was established.

More striking results were obtained upon addition of the above-mentioned anions to **7** or **8**. Thus, **7** underwent an instantaneous blue to orange color change upon addition of 3 mol equiv of F^-.[35] A similar blue to orange color change was observed upon addition of 250 mol equiv of AcO^- anions to **7**, while upon addition of $H_2PO_4^-$ anions, up to 1000 mol equiv, the color of the methylene chloride solution of **7** changed from blue to purple (Figure 2, II). No further color modification could be recorded even upon addition of a large excess of $H_2PO_4^-$ anions to the solution of **7**. As expected, **9a** was also found to be sensitive to the presence of small amounts of fluoride anions, giving rise to an instantaneous blue to pink color change. But, very surprisingly, no change occurred upon addition of very large excess of AcO^- or $H_2PO_4^-$ anions to this compound (Figure 2, III).

Finally, the cationic species **10** behaved quite similarly to complexes **5** and **6**. Indeed, even though **10** showed a pronounced sensitivity to the anions studied (a very fast red to yellow anion color change was induced upon addition of a few molar equivalents of F^-, AcO^-, or $H_2PO_4^-$ anions), no clear distinction between the anions, irrespective to their identities, was detected. Moreover, even addition of Cl^-, Br^-, and HSO_4^- anions resulted in similar color changes (Figure 2, IV).

UV−Visible Spectral Responses of Sensors 5−10. The interaction of the alkynyl ruthenium sensors **5**−**10** with anions was investigated through spectrophotometric titrations, by adding a standard solution of the tetrabutylammonium salt of anions to a dry CH_2Cl_2 solution of sensor. Care was taken to avoid the contamination by water during the preparation of the solution and titration.[13] Compounds **5**−**10** were characterized by very strong absorption bands due to a $d\pi_{(Ru)} \rightarrow \pi^*_{(C\equiv CR)}$ metal-to-ligand charge transfer (MLCT)[36,37] transition in the visible region (**5** $\lambda_{max} = 490$ nm (in methylene chloride); $\epsilon_{max} = 2.5 \times 10^4$ dm^3 mol^{-1} cm^{-1}; **7** $\lambda_{max} = 590$ nm; $\epsilon_{max} = 4.0 \times 10^4$ dm^3 mol^{-1} cm^{-1}). In the presence of anions, the NH−anion hydrogen-bond formation resulted in a blue-shift of this absorption band.

Thiazolidinedione- and rhodanine-based sensors **5** and **6**, which contain only one recognition site, proved to be inefficient in distinguishing between $H_2PO_4^-$, AcO^-, and F^-, respectively. Complete color changes were observed for **5** upon addition of 6 equiv of F^- or 10 equiv of AcO^- (**5**: $\lambda_{max} = 490$ nm; $\epsilon_{max} = 2.5 \times 10^4$ dm^3 mol^{-1} cm^{-1}; [**5.**F^-]- and[**5.**AcO^-]: $\lambda_{max} = 415$ nm; $\epsilon_{max} = 2.3 \times 10^4$ dm^3 mol^{-1} cm^{-1}). The presence of a thiocarbonyl unit in **6** resulted in a higher sensitivity of the sensors and in the lack of discrimination between the anions. The complete color change of the methylene chloride solution of **6** was observed upon addition of 2.5 equiv of AcO^- or 2 equiv of F^-, (**6**:

(35) Commercially available tetrabutylammonium fluoride hydrate.

(36) Powell, C. E.; Cifuentes, M. P.; Morrall, J. P.; Stranger, R.; Humphrey, M. G.; Samoc, M.; Luther-Davies, B.; Heath, G. A. *J. Am. Chem. Soc.* **2003**, *125*, 602−610.

(37) Wong, C.-Y.; Che, C.-M.; Chan, M. C. W.; Han, J.; Leung, K.-H.; Phillips, D. L.; Wong, K.-Y.; Zhu, N. *J. Am. Chem. Soc.* **2005**, *127*, 13997−14007.

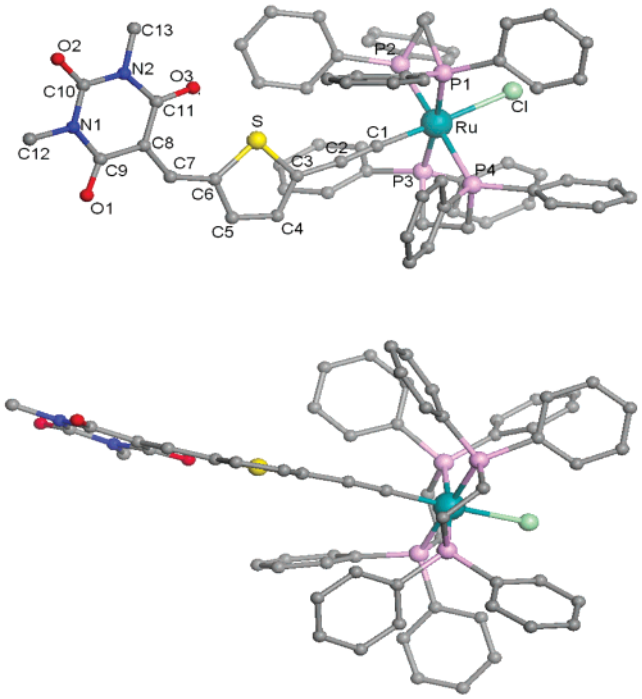

Figure 1. Drawing of complex **9b** in the crystalline state. (a) Top view. (b) Side view. Selected bond distances [Å] and angles [deg]: Ru−C1 1.977-(2), C1−C2 1.204(3), C2−C3 1.406(3), C3−C4 1.386(4), C9−01, 1.218-(4), C11−O3 1.214(3), C10−O2 1.214(4); Ru−C1−C2 177.1(2), C1−C2−C3 174.0(3), Cl−Ru−C1 175.79(6).

λ_{max} = 550 nm; $\epsilon_{max} = 2.6 \times 10^4$ dm^3 mol^{-1} cm^{-1}; [**6**.F$^-$] and [**6**.AcO$^-$]: λ_{max} = 465 nm; $\epsilon_{max} = 2.2 \times 10^4$ dm^3 mol^{-1} cm^{-1}). Moreover, these color changes were not found to be clearly different from those observed in the deprotonation process as monitored by addition of a base (piperidine, potassium *tert*-butoxide, or tetramethyl ammonium hydroxide) which gave rise to a similar yellow solution ([**5**-H$^+$]: λ_{max} = 445 nm; $\epsilon_{max} = 2.2 \times 10^4$ dm^3 mol^{-1} cm^{-1}; [**6**-H$^+$]: λ_{max} = 499 nm; $\epsilon_{max} = 2.1 \times 10^4$ dm^3 mol^{-1} cm^{-1}). These results show that the thiazolidinedione- and rhodanine-based sensors **5** and **6** do not allow deprotonation and hydrogen bonding to be differentiated or discrimination between the anions.

By contrast, the barbituric-based alkynyl ruthenium sensors **7**−**10** discriminate between F$^-$, other anions, and base. Figure 3 shows the UV−vis spectral changes of **7** during the titration with fluoride ions. Upon addition of 1 molar equiv of fluoride ions, little change was observed. However, with the addition of a further amount of fluoride ions, the peak at the λ_{max} of 590 nm disappeared gradually, and a new band grew at 480 nm. The blue color of the sensor solution turned orange. Analogous investigations were carried out on a variety of anions such as $CH_3CO_2^-$, $H_2PO_4^-$, HSO_4^-, Cl$^-$, and Br$^-$. Only $CH_3CO_2^-$ and $H_2PO_4^-$ induced significant spectral changes, but the spectral responses were not as large as those observed for fluoride even with increasing anion concentration. Indeed, 250 molar equiv of AcO$^-$ anions were necessary to induce a similar modification of the spectrum. Finally, even upon addition of large excesses (>1000 molar equiv of $H_2PO_4^-$) the full conversion was never reached with these anions: the system stayed at a stage where both free

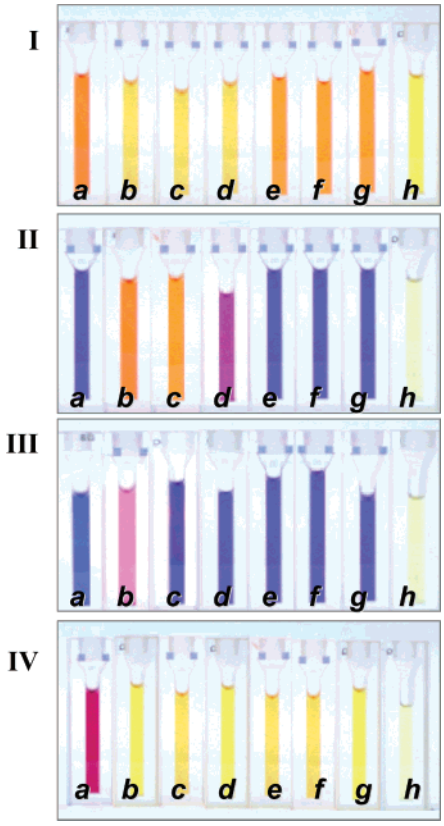

Figure 2. Color changes of 6.7 × 10^{-5} M methylene chloride solutions of selected complexes upon addition of anions as their tetrabutylammonium salts or piperidine. **I**: (a) **2a**, (b) **2a** + 6 equiv of *n*-Bu$_4$NF, (c) **2a** + 20 equiv of *n*-Bu$_4$NAcO, (d) **2a** + 60 equiv of *n*-Bu$_4$NH$_2$PO$_4$, (e) **2a** + 200 equiv of *n*-Bu$_4$NHSO$_4$, (f) **2a** + 200 equiv of *n*-Bu$_4$NCl, (g) **2a** + 200 equiv of *n*-Bu$_4$NBr, (h) **2a** + 10 equiv of piperidine. **II**: (a) **7**, (b) **7** + 4 equiv of *n*-Bu$_4$NF, (c) **7** + 300 equiv of *n*-Bu$_4$NAcO, (d) **7** + 1000 equiv of *n*-Bu$_4$NH$_2$PO$_4$, (e) **7** + 1000 equiv of *n*-Bu$_4$NHSO$_4$, (f) **7** + 1000 equiv of *n*-Bu$_4$NCl, (g) **7** + 1000 equiv of *n*-Bu$_4$NBr, (h) **7** + 40 equiv of piperidine. **III**: (a) **9a**, (b) **9a** + 4 equiv of *n*-Bu$_4$NF, (c) **9a** + 1000 equiv of *n*-Bu$_4$NAcO, (d) **9a** + 1000 equiv of *n*-Bu$_4$NH$_2$PO$_4$, (e) **9a** + 1000 equiv of *n*-Bu$_4$NHSO$_4$, (f) **9a** + 1000 equiv of *n*-Bu$_4$NCl, (g) **9a** + 1000 equiv of *n*-Bu$_4$NBr, (h) **9a** + 50 equiv of piperidine. **IV**: (a) **10**, (b) **10** + 3.5 equiv of *n*-Bu$_4$NF, (c) **10** + 8 equiv of *n*-Bu$_4$NAcO, (d) **10** + 15 equiv of *n*-Bu$_4$NH$_2$PO$_4$, (e) **10** + 100 equiv of *n*-Bu$_4$NHSO$_4$, (f) **10** + 200 equiv of *n*-Bu$_4$NCl, (g) **10** + 200 equiv of *n*-Bu$_4$NBr, (h) **10** + 20 equiv of piperidine.

and complexed receptors would exist. The purple color observed resulted from the concomitant two absorption bands at 590 and 480 nm. Other anions such as HSO_4^-, Cl$^-$, and Br$^-$ did not induce any spectral response.

The barbituric-based anion sensors **7**, **9a**, and **10** behave differently toward anions and base (Figure 3). Indeed, the color changes observed upon addition of F$^-$, AcO$^-$, or $H_2PO_4^-$ anions to complexes **7** leading to orange (F$^-$, AcO$^-$) or purple ($H_2PO_4^-$) colors are clearly different from those observed in the deprotonation process, as monitored by addition of a base (potassium *tert*-butoxide, piperidine, or tetramethylammonium hydroxide) in methylene chloride, which produced a pale yellow solution (λ_{max} = 340 nm; $\epsilon_{max} = 2.2 \times 10^4$ dm^3 mol^{-1} cm^{-1}) (Figure 3d). This color change is consistent with the weakening of the acceptor strength of the barbituric moiety as a result of its deprotonation.[38] Interestingly, while the color changes that were observed

(38) Fillaut, J.-L.; Price, M.; Johnson, A. L.; Perruchon, J. *Chem. Commun.* **2001**, *8*, 739−740.

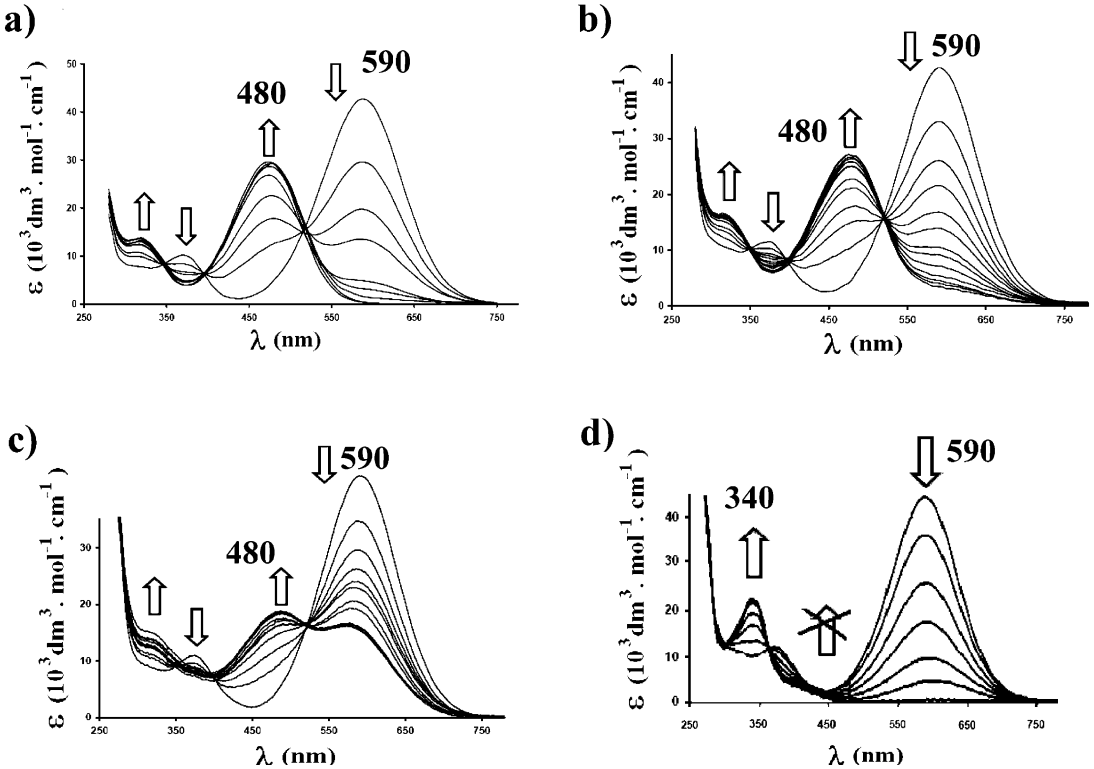

Figure 3. Evolution of the UV−vis absorption spectrum of a 6.7×10^{-5} M solution of **7** in methylene chloride upon addition of increasing amounts of (a) tetrabutylammonium fluoride, (b) tetrabutylammonium acetate, (c) tetrabutylammonium phosphate, and (d) piperidine.

upon addition of F^-, AcO^-, and $H_2PO_4^-$ anions were reversible upon addition of water, the deprotonation process was not affected by the addition of water.

Furthermore, the addition of a huge amount of base (potassium tert-butoxide, piperidine or tetramethyl ammonium hydroxide) to the methylene chloride solution of **7** and 5 equiv of F^- induced a new color change (from orange to pale yellow). This suggests that the complex formed by F^- and the receptor is displaced in favor of the deprotonation of the barbituric head. Taken altogether, these results show that the interactions of the studied anions, especially fluoride anions, with the barbituric-based anion sensors **7**, **9a**, and **10** in poorly polar solvents such as methylene chloride are essentially hydrogen bonding.[39−45]

From the present observations, we can infer some general trends concerning the effect of the presence of two NH sites on deprotonation and hydrogen bonding of various anions (for the investigated sensors). In particular, the simultaneous presence of two NH sites is crucial to induce selectivity between F^-, AcO^-, and $H_2PO_4^-$. It also suggests that this selectivity results from the formation of barbituric complexes with *two* anions.

Barbituric-based sensors **7**, **9a**, and **10**, showed contrasting selectivities toward $H_2PO_4^-$, AcO^-, and F^-. **10** proved to be inefficient for distinguishing between these anions. Complete red to yellow color changes were observed upon addition of 3 equiv of F^-, 10 equiv of AcO^-, or 12 equiv of $H_2PO_4^-$ to this complex (**10**: $\lambda_{max} = 490$ nm; $\epsilon_{max} = 2.4 \times 10^4$ dm^3 mol^{-1} cm^{-1}; [**10.**F^-], [**10.**AcO^-] and [**10.**$H_2PO_4^-$]: $\lambda_{max} = 380$ nm; $\epsilon_{max} = 1.9 \times 10^4$ dm^3 mol^{-1} cm^{-1}).

Conversely, the thienyl derivative **9a** proved to be the most efficient sensor in this series at distinguishing between F^- and the other anions. The complete color change of the methylene chloride solution of **9a** occurred upon addition of 6 equiv of F^-, (**9a**: $\lambda_{max} = 605$ nm; $\epsilon_{max} = 3.5 \times 10^4$ dm^3 mol^{-1} cm^{-1}; [**9a.**F^-]: $\lambda_{max} = 510$ nm; $\epsilon_{max} = 2.2 \times 10^4$ dm^3 mol^{-1} cm^{-1}). Other anions, in particular AcO^- and $H_2PO_4^-$, did not induce any spectral response.

UV−Vis Titration Experiments. Least-squares fitting of the data lead to calculated values of the association constants for the alkynyl ruthenium sensors **5**−**10**. In a typical experiment, a solution of the studied sensor (concentrations ranging from 5×10^{-6} to 5×10^{-5} M) in dry methylene chloride was titrated with increasing amounts of a solution of a tetrabutylammonium salt in methylene chloride (concentration ranging from 5×10^{-4} to 5×10^{-2} M) at room temperature. After addition of each aliquot, the UV−vis spectrum of the solution was recorded from 250 to 900 nm on a Uvikon XL spectrophotometer. The anion-to-sensor ratio was varied from 0 to 300 equiv. When the titration was

(39) Amendola, V.; Bonizzoni, M.; Esteban-Gomez, D.; Fabbrizzi, L.; Licchelli, M.; Sancenon, F.; Taglietti, A. *Coord. Chem. Rev.* **2006**, *250*, 1451−1470.
(40) Amendola, V.; Esteban-Gomez, D.; Fabbrizzi, L.; Licchelli, M. *Acc. Chem. Res.* **2006**, *39*, 343−353.
(41) Boiocchi, M.; Del Boca, L.; Esteban-Gómez, D.; Fabbrizzi, L.; Licchelli, M.; Monzani, E. *Chem. Eur. J.* **2005**, *11*, 3097−3104.
(42) Boiocchi, M.; Del Boca, L.; Gómez, D. E.; Fabbrizzi, L.; Licchelli, M.; Monzani, E. *J. Am. Chem. Soc.* **2004**, *126*, 16507 -16514.
(43) Evans, L. S.; Gale, P. A.; Light, M. E.; Quesada, R. *Chem. Commun.* **2006**, 965−967.
(44) Gale, P. A. *Acc. Chem. Res.* **2006**, *39*, 465−475.
(45) Steiner, T. *Angew. Chem., Int. Ed.* **2002**, *41*, 48−76.

completed, the spectra were imported into the Specfit software.[46] Various stoichiometries were tested according to the number of potential binding sites in the sensor (one or two NH groups), the evolution of the UV−vis spectra was fitted to a model including the formation of the complexeswith one and two anions coordinated to this sensor. For instance, titration of acetate and **7**:

$$7 + AcO^- \underset{k_{-1}}{\overset{k_1}{\rightleftharpoons}} [7.AcO]^- \quad K_1 = k_1/k_{-1}\ (M^{-1})$$

$$7 + AcO^- + AcO^- \underset{k_{-2}}{\overset{k_2}{\rightleftharpoons}} [7.AcO_2]^{2-} \quad K_2 = k_2/k_{-2}\ (M^{-1})$$

Least-squares fitting of the data lead to calculated values of the association constants that were refined with respect to the quality of the fitting parameters and the consistency of the simulated spectra. These binding constants were confirmed for each receptor by using the Letagrop program.[47]

The equilibrium constants were first estimated based on 1:1 (host−guest) binding models for complexes **5**−**6**. The calculated K_1 (Table 2) values for F^-, AcO^-, and $H_2PO_4^-$ anions are qualitatively in agreement with their basicity. These values confirm that complexes **5** and **6** with a sole binding site are definitely not selective. The plots for **7**, **8**, **9a**, and **10** suggest that the stoichiometry of the host−guest complexes is not simply 1:1. Best fits of the UV−vis titration spectra were obtained assuming a 1:2 stoichiometry for the corresponding host−guest complexes. For instance, the plots for **9a** and F^- (see Table 2) give the log $K_1 = 4.0 \pm 0.2$ and log $K_1K_2 = 9.8 \pm 0.3$ for the two-step changes.

The first complexation of F^- and AcO^- anions leads to association constants of rather close values for **7** and **8**, indicating that differences in the intrinsic basicity and electronegativity of the anions are not dominant for the first step changes. Very important differences were observed for the values of the second association constants (**7**: F^-, log $K_2 \approx 6$; AcO^-, log $K_2 \approx 3$) and suggest that the discrimination between fluoride and other anions by **7**, **8**, and **9a** is mainly due to their relative capability to achieve 1:2 host−guest complexes.

Selectivity of the Barbituric-Based Sensors 7−10 toward Anions. Complexes **7**−**9a** discriminate efficiently between fluoride and other anions, while open sensors for fluoride ions generally cannot distinguish F^- from $CH_3CO_2^-$. The differences for the second association constants for complexes **7**−**9a** suggests that their selectivity results mainly from the relative capability of the barbituric-based sensors **7**−**10** to achieve 1:2 host−guest complexes with F^-, AcO^-, and $H_2PO_4^-$. This also suggests that the discrimination between these anions results from modifications of the density of charge in the receptor after complexation of a first anionic species. This behavior can result from several effects. The complexation of a first anion to the receptor will disfavor the complexation of a second anion, as the acidity of the remaining NH site will decrease while the electron density will globally increase. As carbonyl (or thiocarbonyl) groups face incoming anions, it seems reasonable to assume that these groups exert electrostatic repulsions[48−50] over antagonist groups (C═O; P═O). These repulsive effects are obviously enhanced by the complexation of a first anion to the receptor **7**, **8**, or **9a** as the density of electron increases. The higher the electron density at the receptor head, the higher the repulsive effects are and the higher the selectivity is. This behavior particularly disfavors subsequent binding of oxoanions (with C═O or P═O subunits), which are more sensitive than fluoride anions to electrostatic repulsions of neighboring groups as their negative charge is more diffuse.

Table 2. Affinity Constants for Compounds **5**−**10** with Anionic Substrates in Dichloromethane at 22 °C

compound	F^-	AcO^-	$H_2PO_4^-$
5			
log K_1	5.2 ± 0.1	5.0 ± 0.1	4.2 ± 0.1[a]
6			
log K_1	6.7 ± 0.2	7.1 ± 0.4	nd[b]
7			
log K_1	4.2 ± 0.1[a]	4.0 ± 0.1	3.4 ± 0.1
log $K_1.K_2$	10.6 ± 0.1	7.1 ± 0.2	nd[c]
8			
log K_1	4.7 ± 0.1[a]	4.6 ± 0.1	4.4 ± 0.1
log $K_1.K_2$	11.2 ± 0.1	8.8 ± 0.2	7.6 ± 0.3
9a			
log K_1	4.0 ± 0.2[a]	—[d]	—[d]
log $K_1.K_2$	9.8 ± 0.3		
10			
log K_1	5.9 ± 0.1[a]	5.7 ± 0.1	5.6 ± 0.1
log $K_1.K_2$	11.2 ± 0.2	11.0 ± 0.1	10.5 ± 0.2

[a] Maximal values. [b] Nondetermined because of competitive deprotonation; [c] The second equilibrium was suppressed during the fitting process because of the very low concentration of $[7.(H_2PO_4)_2]^{2-}$. [d] See text

Solvation Effects. Surprisingly, fluoride complexation to **7**, **8**, and **9a** shows positive cooperativity ($K_2/K_1 > 4$) whereas other anions show rather anticooperative behaviors ($K_2/K_1 < 1$).[51] Positive cooperativity in binding two anions to these neutral hosts in low-polarity media is unexpected. Actually, the solvation effects make it possible to rationalize the observed cooperativity.[52] Our results suggest that the complexation of anions by **7**, **8**, and **9a** involves a delicate balance between hydrogen binding, electrostatic interactions, and solvation effects. Particularly, the interpretation of these experimental results should necessarily include effects from solvation and desolvation of both anions and receptor, which may be significant.[53,54] At first, incoming anions compete with the solvent molecules that interact with the NH sites. Then, anions when interacting with the NH sites also disturb the interaction of the receptor with solvent molecules: it is

(46) Binstead, R. A. J. B.; Zuberbuhler, A. D. *Specfit/32 Global Analysis System*; Spectrum Software Associates: Chapel Hill, NC, 2000.
(47) Sillen, L. G.; Warnquist, B. *Ark. Kemi* **1968**, 31, 315−339; 337−390.
(48) Beijer, F. H.; Sijbesma, R. P.; Vekemans, J.; Meijer, E. W.; Kooijman, H.; Spek, A. L. *J. Org. Chem.* **1996**, *61*, (6371−6380).
(49) Desiraju, G. R. *Acc. Chem. Res.* **2002**, *35*, 565−573.
(50) Schmuck, C.; Machon, U. *Chem. Eur. J.* **2005**, *11*, 1109−1118.
(51) Connors, K. A. *Binding Constants: The Measurement of Molecular Complex Stability*; John Wiley and Sons: New York, 1987.
(52) A referee suggested considering the possibility that the host could be self-associated to explain this behaviour. NMR studies with compound **7** were performed at various concentrations, but they do not show significant downfield shift of the NH proton as would be expected in such a case.
(53) Beer, P. D.; Gale, P. A. *Angew. Chem., Int. Ed.* **2001**, *40*, 487−516.
(54) Bieske, E. J. *Chem. Soc. Rev.* **2003**, 231−237.

expected that the acidity of the remaining −NH binding site decreases, while the electron density of the carbonyl groups increases, contributing to enhance attractive forces toward solvent molecules. Such changes in the solvation effects will greatly influence the thermodynamic stability of the [1:1] and [1:2] complexes. This is particularly true for the fluoride anions which strongly interact with the −NH binding groups, as the smallest and the most electronegative ions in the studied series.

Modifications of the Alkynyl Ruthenium Moiety and Selectivity. The experimental behavior of **7**, **9a**, and **10** upon interaction with fluoride, acetate, and phosphate suggests the selectivity of the barbituric-based sensors can be tuned by changing the electronic properties of the substituent on the organometallic moiety. **10**, which bears the less electron-donating substituent, experienced similar spectral changes (from 490 to 380 nm) upon interaction of both anions. As expected, the introduction of a nitrile ligand enhances the overall electrostatic attraction of the receptor while it allows the reduction of the electron density of the barbituric ring and the increase in the acidity of the hydrogen-bond donors. Experimentally, we observed an improved sensitivity toward all the anions and a lower selectivity. Indeed, compared to **7** and **8**, or **9a**, the spectrum of **10** was fully modified upon addition of few molar equiv of both anions (F^-, 3 molar equiv; AcO^-, 10 molar equiv; $H_2PO_4^-$, 12 molar equiv). Cl^-, Br^-, and HSO_4^- anions also induced spectral changes, even if the spectral responses were not so sensitive with the increase of anion concentrations. For instance, 20 molar equiv of Cl^- anions were sufficient to induce a total modification of the spectrum. Finally, with the addition of a large amount of anions, the peak at the λ_{max} of 380 nm also gradually disappeared with time, while a band grew up at 590 nm that is in agreement with the slow formation of **7** for instance, with chloride anions. However, the processes when the anions simply bind to the ruthenium, replacing the benzonitrile ligand in **10**, are considerably slower (several hours to go to completion) than that observed because of hydrogen-bonding interactions (few seconds).

Conversely, **9a** bears the most electron-donating substituent in the series. The expected effect is a diminution of the acidity of both NH sites and an increase of the electron density on the neighboring carbonyl sites. These effects result in a lower sensitivity toward anions (**7**/F^-: $\log K_1.K_2 = 10.6$; **9a**/F^- : $\log K_1.K_2 = 9.8$), together with an increased selectivity. In particular, **9a** experiences spectral changes (from 602 to 530 nm) only upon addition of fluoride anions: no detectable color change was observed even upon addition of large excesses of AcO^-, $H_2PO_4^-$, or other anions to this complex. This result shows that the selectivity of the alkynyl ruthenium-based sensors can be improved through electronic modifications of the alkynyl ruthenium moiety.

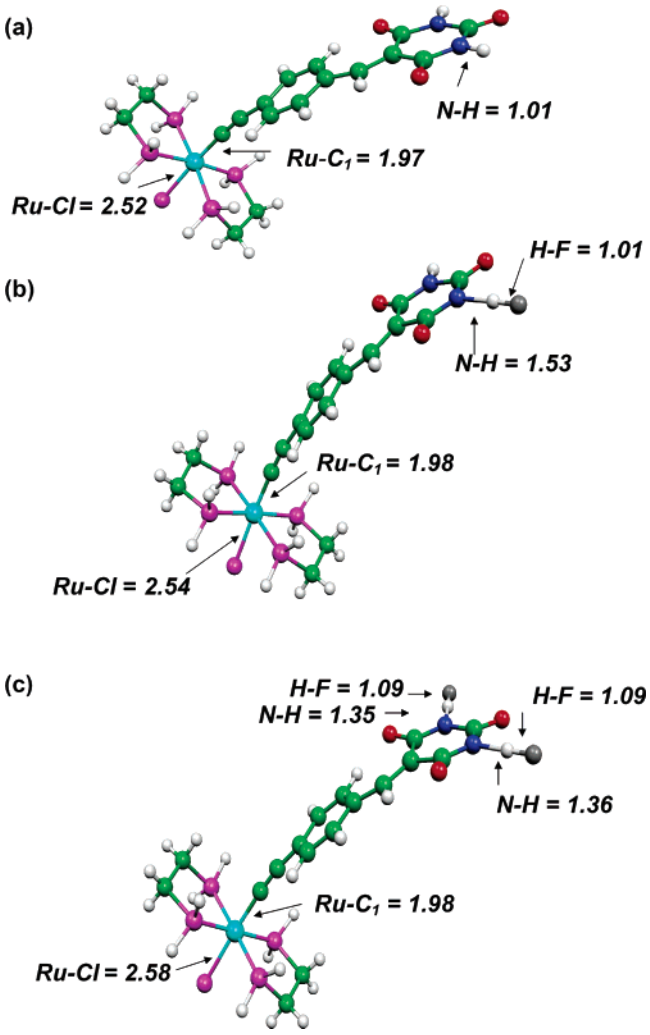

Figure 4. Optimized geometries of **7′** (a), **7′.F**$^-$ (b) and **7′.(F**$^-$**)$_2$** (c). The most significant interatomic distances are given in Å.

Theoretical Analysis. Interactions of the Anions with Barbituric-Based Sensors. DFT calculations were performed on the simplified model **7′** and its fluoride complexes **7′.F**$^-$ and **7′.(F**$^-$**)$_2$** (see computational details in Supporting Information). In these models, dppe (diphenylphosphinoethane) ligands were replaced by $H_2P-(CH_2)_2-PH_2$ phosphines. Full geometry optimizations of **7′.F**$^-$ and **7′.(F**$^-$**)$_2$** lead to the molecular structures shown in Figure 4. The optimized geometry of **7′** (Figure 4a) is in rather good agreement with that obtained by X-ray diffraction for **9b**. The calculated Ru−C and C≡C bond lengths and Ru−C≡C angle (172°) lie in the range of classical values for similar complexes.[30−33,36,55−63] Similarly, the metrical parameters

(55) McDonagh, A. M.; Humphrey, M. G.; Samoc, M.; Luther-Davies, B. *Organometallics* **1999**, *18*, 5195−5197.
(56) McDonagh, A. M.; Humphrey, M. G.; Samoc, M.; Luther-Davies, B.; Houbrechts, S.; Wada, T.; Sasabe, H.; Persoons, A. *J. Am. Chem. Soc.* **1999**, *121*, 1405−1406.
(57) Naulty, R. H.; McDonagh, A. M.; Whittall, I. R.; Cifuentes, M. P.; Humphrey, M. G.; Houbrechts, S.; Maes, J.; Persoons, A.; Heath, G. A.; Hockless, D. C. R. *J. Organomet. Chem.* **1998**, *563*, 137−146.
(58) Powell, C. E.; Cifuentes, M. P.; McDonagh, A. M.; Hurst, S. K.; Lucas, N. T.; Delfs, C. D.; Stranger, R.; Humphrey, M. G.; Houbrechts, S.; Asselberghs, I.; Persoons, A.; Hockless, D. C. R. *Inorg. Chim. Acta* **2003**, *352*, 9−18.
(59) Rigaut, S.; Maury, O.; Touchard, D.; Dixneuf, P. H. *Chem. Commun.* **2001**, 373−374.
(60) Rigaut, S.; Monnier, F.; Mousset, F.; Touchard, D.; Dixneuf, P. H. *Organometallics* **2002**, *21*, 2654 -2661.
(61) Touchard, D.; Haquette, P.; Daridor, A.; Romero, A.; Dixneuf, P. H. *Organometallics* **1998**, *17*, 3844−3852.

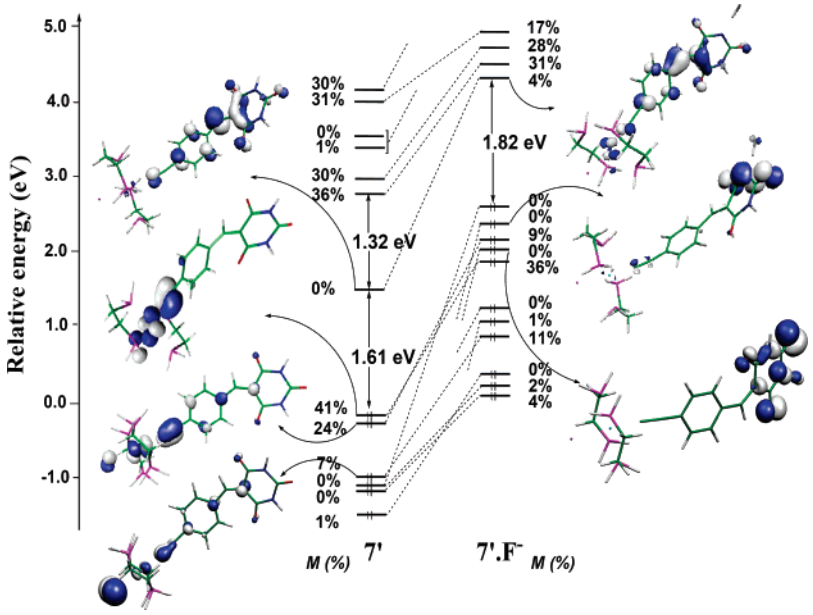

Figure 5. MO Diagrams of **7′** and **7′.F**$^-$

associated with the methylene-barbituric moiety are comparable to those generally observed in related compounds.[38,64,65] These calculations show that the best site for the complexation of the anions is, not surprisingly, located at one of the NH sites of the barbituric unit (Figure 4b). It was not possible to differentiate between the two NH sites however. The N−H−F arrangement is almost linear (177°). The optimized H−F distance is very short (1.01 Å). This distance is only slightly longer than that computed at the same level of theory for the HF molecule (0.92 Å). Consistently, the corresponding N−H bond is considerably weakened upon complexation, its distance going from 1.01 Å in **7′** to 1.53 Å in **7′.F**$^-$. The fluorine atoms in **7′.(F**$^-$**)$_2$** are less strongly bonded than the single one in **7′.F**$^-$. The H−F distance varies from 1.01 Å in **7′.F**$^-$ to 1.09 Å in **7′.(F**$^-$**)$_2$** whereas the corresponding N−H distance is considerably shortened from 1.53 to 1.36 Å.

These calculations allow us to get a more precise view on the inherent properties of the barbituric based sensors toward anions; even thought they cannot fully take into account all the experimental conditions, these calculations allow the communication from the receptor to the alkynyl ruthenium subunit to be highlighted. Indeed, the complexation of F$^-$ has a long-range action and is felt as far as the alkynyl ruthenium subunit. The addition of a fluoride on one barbituric N−H site not only results in a local geometrical effect that would be restricted to the barbituric receptor but also results in geometrical modifications around the ruthenium atom, as exemplified by the lengthening of the Ru−C and Ru−Cl bond distances upon complexation (Figure 4a,c). The addition of a second fluoride on the second barbituric N−H site has qualitatively a similar effect (Figure 4c). These results highlight the efficiency of the long-range electronic communication from the receptor to the alkynyl ruthenium subunit as a main contribution for these sensors.

Changes in the Visible Spectrum upon Complexation of Fluoride Anions. The MO diagrams of **7′** and **7′.F**$^-$ are shown in Figure 5 together with the MO percentage in metal localization. Plots of the HOMO and LUMO of **7′** are also shown. The HOMO has a large metal participation and has no localization on the barbituric moiety. It can be identified as one of the so-called "t_{2g}" components of the octahedrally coordinated Ru(II) center. It is of σ-type with respect to the conjugation "plane" of the organic part of the molecule. It has significant Ru−C antibonding character, as usually observed for HOMOs of related alkynyl complexes.[66] The HOMO-1 lies just below the HOMO. It is of π-type with respect to the conjugation "plane" of the organic moiety. Being mainly localized on the organometallic part of the complex (Cl, 7%; Ru, 24%; C≡C, 29%), it has little localization on the barbituric end of the complex. The HOMO-2 has similar π-type symmetry as the HOMO-1. It can be identified as a Cl lone pair with some weak Ru and C_2 participation. The LUMO of **7′** lies in the middle of a large energy gap separating the "t_{2g}"-type HOMO from the d-type antibonding metal−ligand orbitals (the so-called "e_g*" set). It is a moderately antibonding π-type orbital associated with the organic part of the molecule, having significant localization of the barbituric ring.

The complexation of **7′** by F$^-$ induces a destabilization of all the **7′** MOs. The rationalization of this effect can be approximated as the result of a negative point-charge effect induced by the fluoride ion. This effect is different from that associated with orbital overlap which affects only a couple

(62) Whitall, I. R.; Cifuentes, M. P.; Costignan, M. J.; Humphrey, M. G.; Goh, S. C.; Skelton, B. W.; White, A. H. *J. Organomet. Chem.* **1994**, *471*, 193−199.
(63) Winter, R. F. *Eur. J. Inorg. Chem.* **1999**, 2121−2126.
(64) Deans, R. C.; Cuello, A. O.; Gallow, T. H.; Ober, M.; Rotello, V. M. *J. Chem. Soc. Perkin Trans. 2* **2000**, 1309−1313.
(65) Li, Y.; Snyder, L. B.; Langley, D. R. *Bioorg. Med. Chem. Lett.* **2003**, *13*, 3261−3266.
(66) Bruce, M. I.; Low, P. J.; Costuas, K.; Halet, J. F.; Best, S. P.; Heath, G. A. *J. Am. Chem. Soc.* **2000**, *122*, 1949−1962.

of N−H σ-type orbitals. The latter is a bond-localized effect, while the former acts at longer distances. However, the shorter the distance, the stronger the point-charge destabilization is. Therefore, the HOMO of **7′** being localized far from F in **7′**.$\mathbf{F}^-$, it is much less destabilized than the LUMO of **7′**, which has significant localization on the barbituric end of the complex. It results that the gap separating these two orbitals increases considerably (Figure 5). It turns out that the HOMO of **7′** is no more the HOMO of **7′**.$\mathbf{F}^-$ because other occupied MOs of **7′** which have larger localization on the organic part of the molecule afford a larger destabilization upon F^- complexation. Nevertheless, the HOMO/LUMO gap of **7′**.$\mathbf{F}^-$ is larger than that of **7′** due to the very strong destabilization of the **7′** LUMO. From these results, one can anticipate a blue-shift upon F^- complexation of the optical transitions involving the frontier orbitals of F^-. Such an effect is consistent with the change in the visible spectrum of **7** upon F^- complexation (see above).

TD-DFT calculations[67] on **7′** and **7′**.$\mathbf{F}^-$ provide a descriptive interpretation of the optical properties of the alkynyl ruthenium-based sensors **7**−**10** and highlight the long-range electronic communication as a main characteristic of the alkynyl ruthenium species (see computational details in Supporting Information). In the case of the uncomplexed compound **7′**, the two transitions of lowest energy were computed (solvent corrections considered) for $\lambda = 699$ nm (oscillator strength = 0.38) and $\lambda = 582$ nm (oscillator strength = 0.46). Obviously, the discrepancy with respect to the corresponding experimental values (588 and 375 nm, respectively) is quite large and can be attributed to the intrinsic limitations of our level of modelization. In particular, it is known that TD-DFT calculations of adiabatic long-range charge-transfer excitation energies (see below) are underestimated with respect to the observed transition values.[68,69] The calculated transition at 699 nm is not far from the red edge of the observed absorption band and thus may not be as far off the experimental value as suggested. The calculated band at 582 nm is far from the observed band at 375 nm and also has a much larger oscillator strength than would be expected from the observed extinction coefficient. Although it looks smooth in Figure 2, it cannot be excluded that a second band would be lying under the large lower-energy broad peak.

Nevertheless, a qualitative analysis of the transitions and of their shifts upon complexation of **7′** by F^- is possible, as described hereafter. The 699 nm wavelength is associated with a transition from the HOMO-1 to the LUMO. A minor contribution of the HOMO-2 is also computed. Thus, this transition can be described as corresponding to a transfer from the organometallic end to the barbituric end of the molecule. This is a π(ligand + metal) to π(ligand) transition. The 582 nm wavelength is associated with a transition from the HOMO-2 to the LUMO. A minor contribution of the HOMO-1 is also computed. Thus, this π(ligand) to π(ligand) transition is also associated with a transfer from the organometallic end to the barbituric end of the molecule.

In the case of the **7′**.$\mathbf{F}^-$ complex, the two transitions of lowest energy are computed for $\lambda = 661$ nm (oscillator strength = 0.46) and $\lambda = 529$ nm (oscillator strength = 0.29). Both wavelengths are associated with transitions from linear combinations of the HOMO-1 and HOMO-3 to the LUMO. The HOMO-1 and HOMO-3 are associated with π-type nitrogen and oxygen lone pairs of the barbituric unit (Figure 5). The participation to these two transitions of occupied MOs localized on the organometallic moiety is negligible.

Thus, our theoretical calculations indicate that the optical blue-shift observed upon complexation of **7′** by F^- does not correspond to a simple shift in energy of the frontier orbitals but results from a change in their nature due to the point charge effect of the fluoride anion. This effect induces level crossings, which in turn change the optical transitions. It appears that this theoretical analysis does not allow a quantitative interpretation of the whole experimental system we studied. Because of limitations in these calculations, it is obviously difficult to assume that our model can fully take into account all the experimental conditions. In particular, solvent effects are approximated to a continuum and are unable to mimic the first solvation shells of the ions. Nevertheless, our model allows a descriptive interpretation of the optical properties of the alkynyl ruthenium colorimetric sensors **7**−**10** and provides a qualitative analysis of the transitions and of their shift upon complexation of **7′** by F^-. This theoretical model highlights also the long-range electronic communication as a main characteristic of the alkynyl ruthenium species and it consolidates our interpretation of why the selectivity of the alkynyl ruthenium-based sensors is sensitive to electronic modifications of the alkynyl ruthenium moiety.

Conclusions

We have demonstrated that the alkynyl ruthenium may serve as sensitive and selective colorimetric sensors for anions, based on the attachment of rhodanine and barbituric units as recognition centers at the remote end of alkynylruthenium donor-π-acceptor derivatives. Addition of anions to dichloromethane solutions of these alkynyl ruthenium sensors results in instantaneous color changes. Experimental and computational studies indicate that these color changes result from complexation of the anions at the recognition NH sites of the receptors. These color changes were ascribed to authentic hydrogen binding. Interestingly, the simultaneous presence of two NH sites at the recognition center in barbituric derivatives **7**, **8**, and **9a**, and the subsequent formation of complexes with two anions are crucial to induce selectivity between F^- and the other anions in these sensors. The selectivity of these ruthenium derivatives for F^- over $CH_3CO_2^-$ and other anions is not only due to the suitable acidity of their NH groups but also to repulsive effects of the neighboring carbonyl sites of the barbituric head: the higher the electron density at the receptor head, the higher

(67) te Velde, G.; Bickelhaupt, F. M.; van Gisbergen, S. J. A.; Fonseca, Guerra, C.; Baerends, E. J.; Snijders, J. G.; Ziegler, T. *J. Comput. Chem.* **2001**, *22*, 931−967.
(68) Gritsenko, O.; Baerends, E. J. *J. Chem. Phys.* **2006**, *121*, 655−660.
(69) Neugebauer, J.; Gritsenko, O.; Baerends, J. E. *J. Chem. Phys.* **2006**, *124*, 214102.

the selectivity is. As a consequence, the selectivity toward the anions, particularly the fluoride anions, can be finely tuned by changing the electronic properties of the alkynyl ruthenium subunit. DFT calculations rationalize the long-range electronic communication as a main characteristic of the alkynyl ruthenium species and as a key to improve the selectivity of these alkynyl ruthenium-based sensors toward anions.

Acknowledgment. The authors thank the French Ministry of Research, la Région Bretagne, and CNRS for financial support. Computational facilities were provided by the IDRIS (Orsay) and CINES (Montpellier) centers.

Supporting Information Available: Experimental procedures and characterization data for compounds **2**−**10**. Experimental data for UV−vis titration experiments; crystal data, X-ray structure refinement details for **9b**; and computational details. This material is available free of charge via the Internet at http://pubs.acs.org.

IC062389I